Journal of Power Sources 228 (2013) 151–158

Contents lists available at SciVerse ScienceDirect

Journal of Power Sources

journal homepage: www.elsevier.com/locate/jpowsour

Electron beam patterned Nafion membranes for DMFC applications

Ayokunle Omosebi*, Ronald S. Besser

Department of Chemical Engineering and Materials Science, Stevens Institute of Technology, Castle Point on Hudson, Hoboken, NJ 07030, USA

HIGHLIGHTS

- ► Performance evaluation of EBL and dry etching patterned Nafion 212 membranes.
- ► Comparison to pristine, electron beam exposed, and O_2 plasma treated Nafion.
- ► Chemical modification and interfacial enlargement improve performance.
- ► Significantly improved performance results for patterned DMFC.
- ► Comparison of patterned N212 and pristine N117 DMFCs.

ARTICLE INFO

Article history:
Received 2 August 2012
Received in revised form
5 November 2012
Accepted 21 November 2012
Available online 28 November 2012

Keywords:
DMFC
Electron beam lithography
Nafion patterning
Nafion lithography
Methanol crossover

ABSTRACT

Patterned Nafion 212 membrane prepared by electron beam lithography (EBL) coupled with dry etching was tested for DMFC applications. Pristine, O_2 blanket-etched, and electron beam exposed Nafion 212 test cells were also prepared and compared. Several parameters including in-plane conductivity, methanol crossover, *I–V* characteristics, and through-plane ohmic resistance were evaluated. The patterned membrane had the best combination of properties, benefiting from the exposure to electron beam and interfacial area enlargement as evidenced by its superior power density. The maximum power densities were 29.3, 32.5, 48.2, and 63.1 mW cm^{-2} for the pristine, exposed, O_2 blanket-etched, and patterned membrane respectively. A Nafion 117 membrane test cell was also compared. While it exhibited reduced methanol crossover, it also had higher ohmic resistance and Tafel slope. The patterned Nafion 212 provided a 25% increase in power density compared to the N117 membrane.

1. Introduction

Direct methanol fuel cells (DMFCs) produce DC potential from the methanol and oxygen oxidation–reduction reactions occurring at the respective anode and cathode sides a membrane, usually Nafion. DMFCs are attractive alternatives to conventional power sources, particularly for portable applications. Continued interest in DMFCs stems from their many attributes, including efficiency, quiet operation, and simplicity [1–3]. Additionally, methanol is a high energy density fuel that is relatively inexpensive and easy to transport and store. So far, the wide-scale commercialization of the DMFC has been impeded by the high cost of materials used in its construction and performance losses. The loss in performance results primarily from anode-to-cathode methanol crossover and the slow reaction kinetics of both methanol oxidation and oxygen reduction at the anode and cathode respectively [1,2,4].

Nafion is the most widely used membrane for DMFC construction due to its mechanical stability, facile proton transport, and permeation selectivity [2,5]. Proton transport in Nafion is a strong function of water content whereby the protons are moved along with water flowing through its cluster of ionic channels. Anode-to-cathode methanol permeation results from electro-osmotic drag by the hydrated protons and diffusion [2,6]. To reduce the flux of methanol through the membrane, a thicker Nafion membrane is usually employed. Some mitigation strategies focus on membranes like the sulfonated poly ether ether ketone (SPEEK) and sulfonated poly sulfone (SPSf) that exhibit lower methanol crossover as Nafion replacements for the construction of the DMFC [1,2,7]. Presently, the result of these innovations is a tradeoff between methanol permeation and ionic conductivity. Other approaches have dealt with Nafion treatment to reduce methanol crossover. In the work by Hobson and coworkers, Nafion was blanket exposed to a beam of electrons in a low oxygen concentration system [8]. It was found that depending on exposure dose, Nafion displayed improved performance possibly due to greater resistance to methanol

* Corresponding author. Tel.: +1 201 216 5523; fax: +1 201 216 8306.
E-mail address: aomosebi@stevens.edu (A. Omosebi).

0378-7753/$ – see front matter © 2012 Elsevier B.V. All rights reserved.
http://dx.doi.org/10.1016/j.jpowsour.2012.11.076

crossover or the formation of a carboxylic group attachment which leads to improved conductivity. In a different effort, Choi and coworkers reduced methanol crossover by treating Nafion with argon plasma [9].

Cost reduction is a major driving force for DMFC improvements. The sluggishness of the reactions at the electrodes leads to the requirement of increased catalyst loading and consequently cost. The more important metric is the amount of surface available per gram of catalyst loaded. In order to maximize catalyst utilization, the extent of the reaction zone should be maximized without increasing transport resistance for reactants accessing the reaction plane. To achieve this objective, the membrane–electrode interface could be restructured to possess a larger interfacial area by creating features on the Nafion membrane. Strategies such as plasma roughening [9], hot embossing lithography [4], and nanoimprint lithography [7] have been used to restructure the membrane–electrode interface but have resulted in only modest performance increases for the DMFC. By comparison much more work has been done on Nafion patterning for the proton exchange membrane fuel cell. We recently demonstrated the use of electron beam lithography (EBL) coupled with dry etching for the nano/micro-patterning of Nafion 212 membranes [10].

Electron beam lithography involves the exposure of a directed beam of electrons to an electron sensitive material, followed by the subsequent transfer of the resolved pattern onto an underlying substrate. EBL is a convenient tool for nano/micro pattern creation in Nafion that provides access to features with critical dimension as small as 10 nm, while dry etching allows for aspect ratio manipulation. In comparison to the other tools so far employed for Nafion patterning, EBL presents a pathway for both interfacial area enhancement and Nafion chemical structure modification from energetic electrons. In this communication we present the performance evaluation of electron beam patterned membranes for DMFC applications.

2. Experiment

2.1. Fabrication process

Nafion membranes purchased from fuelcellstore.com were used in this study. In preparation for the fabrication process, Nafion 212 membranes were mounted on a silicon wafer using Kapton tape. A 30 nm thick germanium layer was subsequently deposited as a hard mask using a Lesker PVD-75 sputter coater equipped with a crystal thickness monitor (Lesker gold electrode 6 MHz sensor crystals) for deposition rate and thickness determination. ZEP 520A ebeam resist was spun onto the substrate at 3 krpm for 45 s followed by baking at 70 °C for 2 min. The substrate was exposed using a JEOL 6300FS electron beam system. The nominal dose and current were 150 μC cm^{-2} and 1–8 nA respectively. The exposure time t can be estimated from:

$$t = \frac{Q \times A}{i} \tag{1}$$

where Q, A, and i are the dose (C m^{-2}), exposed area (m^2), and current (A) respectively. Following exposure, the substrate was developed in xylene and subsequently dried using a nitrogen gun. Pattern transfer from the developed resist, through the mask to the Nafion substrate proceeds via multiple etching steps. The etching steps consisted of CHF_3 plasma etch to transfer the pattern in the developed resist layer to the Ge hard mask layer, followed by O_2 etching to transfer the pattern in the mask layer into the Nafion layer. This step also removes all of the resist. A post CHF_3 etch step is performed to remove the masking layer. Additional details of the fabrication process can be found in reference [10]. O_2 and CHF_3 etching were performed in a Trion Phantom III reactive ion etching tool. The verification of pattern geometry was done with a Hitachi SEM, Helios Nanolab SEM/FIB system and DEKTAK surface profilometer. The nominal pattern consisted of 2 μm blind pores with 5 μm pitch, 1:1 aspect ratio, and a pattern density of 4×10^6 cm^{-2}. The superficial surface area enhancement was 1.5 times, i.e., 50% area increase over planar Nafion.

2.2. FTIR/ATR

Chemical structure changes in Nafion were investigated using a Thermo Scientific Nicolet 6700 IR/ATR spectrometer equipped with a “smart miracle” accessory and a ZnSe crystal. Spectral data was collected from 400 to 4000 cm^{-1}, and 64 scans were performed per run. The resolution of the spectrum was 4 cm^{-1}. A background scan is performed prior to scanning or after switching to a new sample, and every 10 min.

2.3. Membrane conductivity testing

In-plane membrane conductivity measurements were done using a BEKKTECH BT-112 conductivity cell. Test Nafion membranes were cut into 1 cm × 3 cm samples. Test cells were conditioned with fully humidified argon gas for 2 h. During conditioning, the cell and humidifier temperatures were preset to 60 °C and the Ar flow rate was 100 sccm. The resistance of the membrane was measured using impedance spectroscopy (PAR 2273 potentiostat). During EIS, the frequency was scanned from 100 mHz to 100 kHz with a signal amplitude of 10 mV RMS. After conditioning, the Ar flow rate was changed to 500 sccm. The resistance was measured with 5–10 min interval between each subsequent measurement. Sample thickness was measured using a high-resolution caliper in conjunction with etch rate information for the etched samples. The membrane's conductivity σ was calculated from resistance data using:

$$\sigma = \frac{L}{R \times A} \tag{2}$$

where L is the distance between the voltage sensing electrodes, R is the measured membrane resistance, and A is the area perpendicular to the direction of measurement.

2.4. Water content

In order to assess the saturated water uptake of the membranes, Nafion samples were dried over hygroscopic silica beads in a convective oven at 80 °C for 3 days. The dried Nafion samples were weighed and then equilibrated in boiling water at 80 °C for 4 h with light stirring. The samples were then equilibrated in water at room temperature for 24 h. The hydrated Nafion is retrieved, and excess water was carefully wiped off prior to weighing the sample. The water content, W_c, is determined from

$$W_c(\%) = 100 \times \frac{(M_w - M_d)}{M_d} \tag{3}$$

where M_w and M_d are the wet and dry Nafion sample weights, respectively [4].

2.5. MEA assembly and testing

Gas diffusion electrodes (GDEs) were fabricated by spraying catalyst-ionomer dispersion onto carbon paper (AvCarbTM

GDS2120). The anode and cathode were Pt/Ru (1:1) dispersed on carbon black and unsupported Pt black respectively with a corresponding loading of 1.9 mg cm^{-2} and 2.0 mg cm^{-2} for the Pt/Ru and Pt black. Membrane electrode assemblies (MEAs) were fabricated by hot-pressing the GDEs to the Nafion membranes using a Carver Model 4388 hot-press equipped with a digital pressure gauge. In this work, the modified side was configured as the cathode. The MEAs were hot-pressed at 135 °C and 13 MPa for 165 s. Each MEA was assembled into a test cell and conditioned with humidified H_2 and O_2 fed to the anode and cathode respectively. The active area of the test cell was 1 cm^2. During conditioning, the anode and cathode flow rate, cell temperature, and humidity were 50 sccm, 60 °C, and 100% RH. A backpressure of 103 kPa was applied to both the anode and cathode feed streams. The cells were conditioned for approximately 12 h at 0.6 V until the current density stabilized. The cell was subsequently purged with Ar, and the fuel was switched to methanol. For DMFC performance testing, 2 M methanol was fed to the anode at 1 ccm, while 100 sccm humidified O_2 was fed to the cathode. The cell temperature was maintained at 60 °C and no backpressure was applied. Polarization data was obtained by scanning the current and recording the voltage response. The conditioning, and performance evaluation of the test Nafion cells were done using a Scribner 850e test system. Methanol flow rate was controlled using a Wellchrom K-1001 HPLC pump, while gas flow rate was controlled by the Scribner test system.

Information on methanol crossover was acquired by performing linear scan voltammetry (PAR 2273). Methanol and Ar were fed to the anode and cathode respectively. The cathode was used as the working electrode, while the anode was both the reference and counter electrode. The potential of the working electrode was swept in the anodic direction from 0 to 1.0 V at a scan rate of 2 mV s^{-1}. The methanol crossing over from the anode is oxidized leading to a current response to the scanned potential. The limiting crossover current was obtained from the linear voltammetry experiment. Likewise, cyclic voltammetry was used to evaluate the available electrochemical active area (ECSA). In this scenario, instead of methanol, hydrogen was fed to the anode, and the potential of the working electrode was swept in the anodic direction from 0 to 1.2 V at a scan rate of 40 mV s^{-1}.

2.6. Membrane modifications

In addition to the patterned membrane, pristine, O_2 blanket-etched, and ebeam exposed membranes were also tested for comparison. The pristine membrane was as-received Nafion without any modification done. The exposed membrane was directly treated with the electron beam without any additional fabrication steps. The exposure process followed the same pattern as the patterned membrane received. O_2 etching was done at a power, pressure, and flow rate of 150 W, 50 mTorr and 50 sccm respectively unless otherwise noted. The corresponding etch rate was 20 nm s^{-1}.

3. Results and discussions

3.1. SEM and optical image analysis of fabricated Nafion

Fig. 1 shows SEM images of pristine, O_2 blanket-etched, and patterned Nafion membranes. The etching process results in increased surface roughness as evident in Fig. 1b. Similar roughness was observed for CHF_3 blanket-etched Nafion (not shown) at similar conditions. The exposure of the membrane to the electron beam does not change surface morphology. Nafion patterning requires a succession of etching steps. The patterned Nafion membrane in Fig. 1c, shows roughness similar to the etched membrane. The roughness in the unexposed (non-pore) regions results from CHF_3 post etching to remove the masking layer, and can be mitigated by performing a hydrogen peroxide cleaning step or reducing the etch duration. Typically in microfabrication, the rough grass-like structure is associated with a micromasking effect [11].

As shown in Fig. 2, optical change due to the etching of the Nafion membrane is visible to the naked eye. Pristine Nafion is a transparent film as shown in Fig. 2a, and the continued etching of

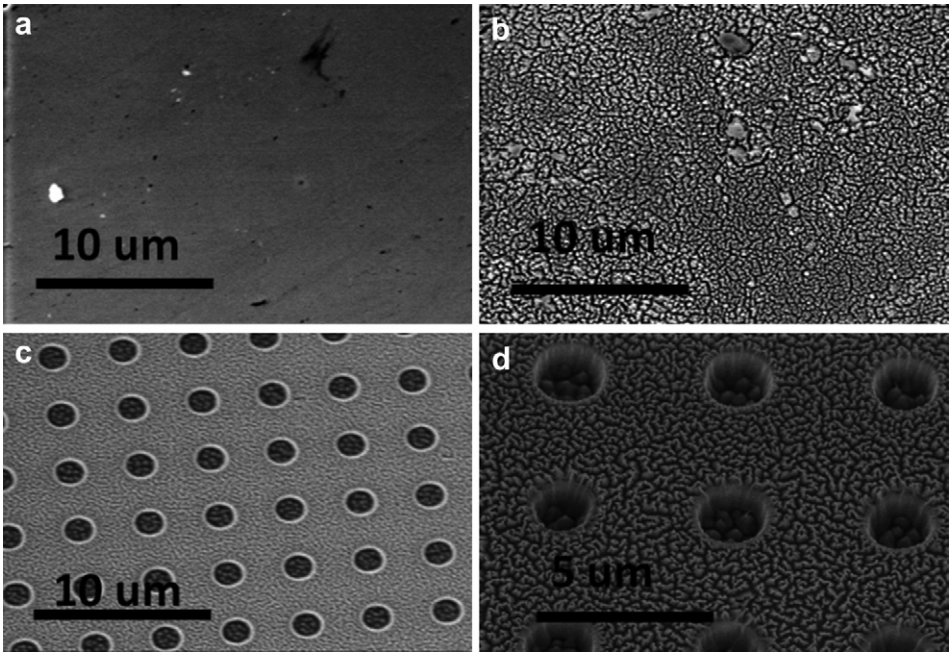

Fig. 1. SEM micrographs of (a) pristine, (b) Blanket-etched, and (c) patterned Nafion 212 membrane. Image (d) is an image of the patterned Nafion 212 membrane at a higher magnification. The patterned structure consisted of blind pores with a critical dimension of 2 μm and 5 μm pitch.

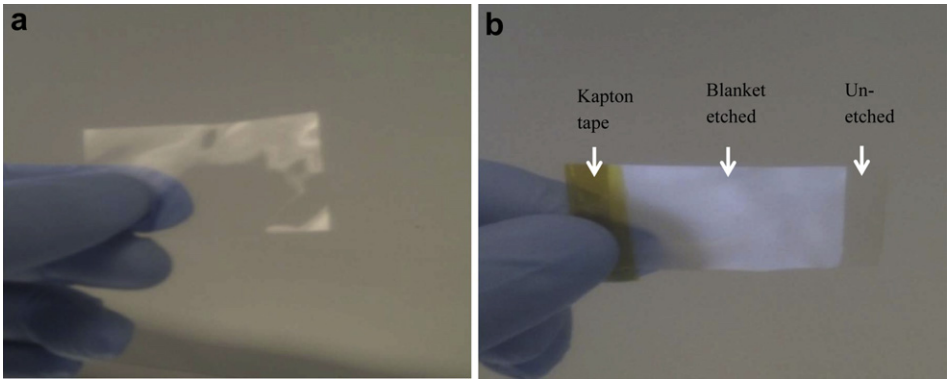

Fig. 2. Optical images of (a) pristine and, (b) Blanket-etched Nafion membranes (color images). (For interpretation of the references to colour in this figure legend, the reader is referred to the web version of this article.)

Nafion results in the membrane becoming opaque with a white-grey tint as shown in Fig. 2b. This transition in opacity could not be replicated by the roughening of Nafion with abrasive paper. One possible explanation of this transition is Nafion becoming more PTFE-like due to the preferential removal of side chain atoms as observed by Kim and coworkers during the etching of Nafion in He plasma [12]. A more PTFE-like membrane should have a reduced conductivity due to a diminished concentration of the sulfonic acid side chains. However, as the modifications to the Nafion are at a surface level, the Nafion bulk should still retain its original properties. Plasma treatment is multifaceted, as it can lead to material deposition as well as removal. In order to investigate possible changes in chemical structure, FTIR/ATR spectroscopy was performed.

3.2. FTIR/ATR studies: effect of fabrication procedure on chemical structure

Fig. 3 shows the spectra of pristine, etched, and patterned Nafion 212 membranes. During etching with either CHF_3 or O_2, 1 μm of Nafion was etched away from the surface. The prominent peaks are identified in Table 1. The spectra show chemical species preservation for the studied membranes with the exception of the peak at 1770 cm^{-1} for the patterned membrane. This peak can arise from the formation of $-CF = CF_2$, $-RC = CF_2$, or $-C{=}O$ bonds as a result of the exposure of Nafion to the electron beam [8]. The resulting structure can affect the properties of Nafion, such that $-RC = CF_2$ or $-CF = CF_2$ formation lead to decreased conductivity due to their hydrophobic nature, while $-C{=}O$ formation results in increased conductivity for the membrane, since the electronegative oxygen can provide a site for proton conduction.

A reduction in signal intensity can also be seen in the spectra for the major peaks of the O_2 and CHF_3 blanket-etched, and patterned samples. Following from the discussion of Fig. 2, if etching were to result in the membrane becoming more PTFE-like, then the ratio of the intensity of the $-SO_3$ peaks to the $-CF$ peaks should tend towards zero as PTFE does not contain $-SO_3H$. However this was not observed from the spectra. The same conclusion was drawn from the spectrum of an O_2 plasma deep-etched Nafion sample. This sample was etched for a longer duration to remove 10 μm of Nafion. When using a ZnSe crystal support substrate for ATR spectroscopy, the penetration depth of the evanescent wave into the sample is typically between 0.5 and 5 μm [15] and good contact is required between the crystal and the sample [16]. The observed changes to the surface character from the patterning of Nafion as illustrated in Fig. 1, affects the nature of the contact between the sample and the ATR crystal which likely explains the observed differences in signal intensity.

3.3. Effect of Nafion modification on in-plane conductivity

Fig. 4 shows the effect of surface treatment on the in-plane conductivity of ebeam exposed, pristine, O_2-etched Nafion 212

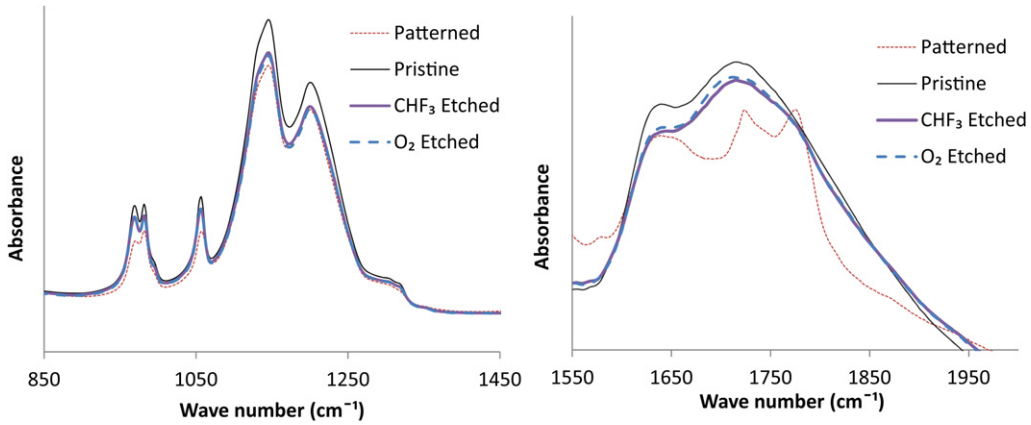

Fig. 3. FTIR/ATR scans for pristine, O_2 and CHF_3 blanket-etched, and patterned Nafion membranes. Etching was done to remove approximately 1 μm of Nafion from the surface. The pressure, flow rate and power for the O_2 plasma were 50 mTorr, 40 sccm, and 80 W respectively, while those for the CHF_3 plasma were 30 mTorr, 50 sccm, and 80 W respectively.

Table 1
Peak assignments for the prominent species in the FTIR/ATR spectra of Nafion.

Wave number (cm^{-1})	Assignment
966, 980	−COC− symmetric stretching [13,14]
1055	$-SO_3-$ symmetric stretching [13,14]
1160, 1200	$-CF_2-$ symmetric stretching [13,14]
1630, 1700	H−O−H bending [13,14]
1770	$-CF=CF_2$ or $-RC=CF_2$ or −C=O vibrations [8]

membranes. O_2 etching was done to remove approximately 1 μm of Nafion. The exposed membrane exhibited the largest in-plane conductivity, while no major change in conductivity was observed in the other membranes due to the modification. This increase in conductivity of the ebeam exposed Nafion supports the hypothesis that carboxylic group formation is the result of the electron beam treatment (Fig. 3). This result is consistent with the observations made by Hobson and coworkers for blanket electron beam irradiated membranes [8].

3.4. Effect of Nafion modification on water content

It is well known that ionic conductivity in Nafion is strongly dependent on water content [17]. Fig. 5 shows the result of the water content experiment for pristine, O_2-etched, exposed, and patterned Nafion 212 membranes. The result shows insignificant change in water content as a result of the modifications made to the membrane. This implies that the ebeam exposure does not change the volume available for water uptake in Nafion, but only effects a change in conductivity as a result of the chemical modification.

3.5. Effect of Nafion modification on ECSA

Fig. 6 shows the cyclic voltammogram for exposed, O_2-etched, pristine, and patterned Nafion 212 membranes. The plot shows overlapping CV curves for the tested membranes indicative of a similar catalyst loading. The electrochemical surface areas (ECSA) determined from the CV curves were 19.2, 19.1, 18.9, 19.2 $m^2\ g^{-1}$ for the O_2-etched, exposed, patterned and pristine membranes respectively. The spread in data represents a deviation of 0.3 $m^2\ g^{-1}$, which is within the error margin for this measurement.

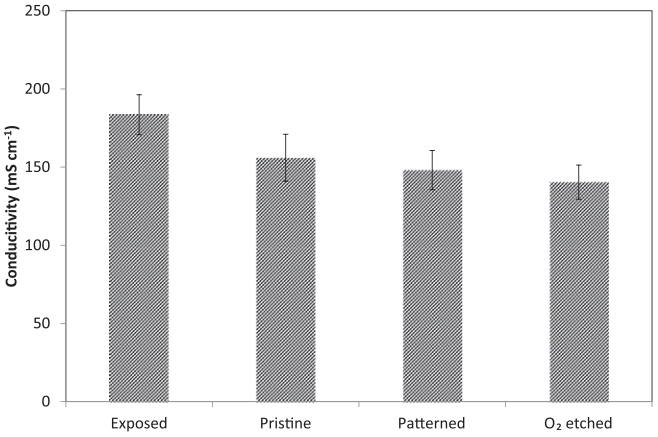

Fig. 4. In-plane conductivity of exposed, pristine, patterned and O_2-etched Nafion membranes. O_2 etching was performed to remove 1 μm from the Nafion surface. The error bars represent ±3 times the standard deviation of measurements performed 7 or 8 times.

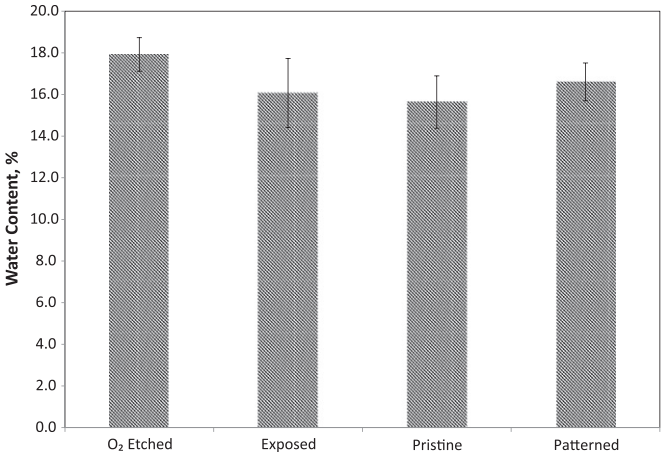

Fig. 5. Water content of pristine, O_2-etched, exposed, and patterned Nafion 212 membranes. The error bars represent ±3 times the standard deviation of measurements performed three times.

3.6. Effect of Nafion modification on ohmic resistance

Fig. 7 shows the through-plane ohmic resistances for pristine, O_2-etched, exposed, and patterned Nafion 212 membranes as a function of current density. The data was collected in-situ and via the current interrupt method. Here we observe that pristine Nafion shows a significantly increased resistance in comparison to the other membranes. For example, at a current density of 125 mA cm^{-2}, the membrane resistances were 81.1, 86.1, 93.5, and 120.1 mΩ cm^2 for the O_2-etched, patterned, exposed, and pristine membranes respectively.

Unlike the in-plane configuration, through-plane membrane resistance measurements are affected by the series resistances of the flow field, gas diffusion media, and interfaces, since the measurement is carried out in a complete fuel cell structure [18]. A key difference between the tested membranes, which can impact series resistance, is the nature of the membrane–electrode interface. Both pristine and exposed membrane cells have flat 2-D interfaces, while the etched and patterned membrane cells possess structured interfaces. We believe that the reduction in resistance in the etched membrane was accomplished via a combination of membrane thinning and increased contact area from surface roughening. For the exposed membrane, the reduction in resistance

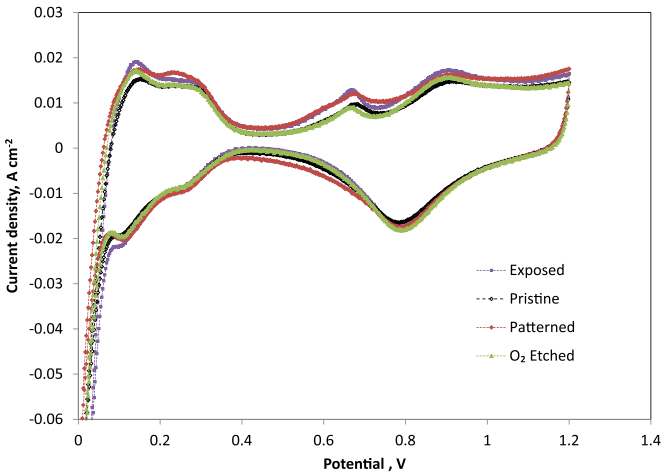

Fig. 6. Cyclic voltammetry scans for pristine, O_2-etched, exposed, and patterned Nafion 212 membranes.

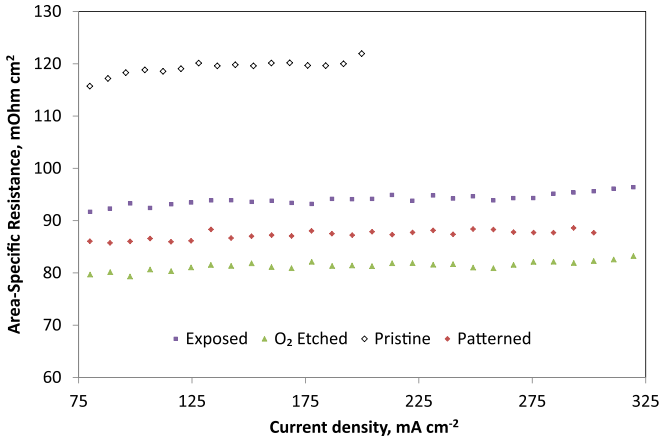

Fig. 7. Through-plane area-specific resistance of pristine, O_2-etched, exposed, and patterned Nafion 212 membranes determined by the current interrupt technique.

is a result of the change in chemical structure, as evidenced by the emergence of the carboxylic group peak at 1770 cm^{-1} from the FTIR/ATR spectra peak in Fig. 3. The reduced resistance of the patterned membrane is a combination of the effects of both ebeam treatment, and interfacial area enlargement.

3.7. Effect of Nafion modification on the methanol crossover

Methanol crossover is perhaps the biggest problem facing DMFCs. Fig. 8 shows the methanol crossover data acquired for pristine, O_2-etched, exposed, and patterned Nafion 212 membranes obtained via linear voltammetry experiments. The exposed membrane exhibited the lowest crossover current density. The maximum crossover currents were 108.8, 120.1, 135.9 and 145.6 mA cm^{-2} for the exposed, pristine, patterned and etched membrane respectively. Resistance to methanol crossover generally scales with membrane thickness. However, the etched membrane has a thickness reduction of only approximately 2% in comparison to the pristine membrane, hence this cannot completely explain the trend between curves a and c in Fig. 8. The etching results obtained here did not agree with the work by Choi and coworkers who found a decrease in methanol permeation as a result of etching [9]. However the work in [9] was performed under different conditions and with different etching gases.

The process of exposing Nafion to the electron beam leads to competing processes of hydrophilic side chain removal and the formation of $-CO_2H$ groups generated within the polymer [8]. Due to the superficial nature of the exposure process, the unaffected parent material is still available to conduct protons. The formation of a methanol-blocking layer at the surface incident to the beam can lead to reduced methanol crossover, which will be consistent with the results for the exposed membrane in Fig. 8. Conversely, with respect to the surface-enlarged membranes, i.e., etched and patterned, their enlarged areas would provide access to a higher flux of methanol.

Since the membrane–electrode interface is the generation/recombination zone for the different species involved in current production, the material properties that result from the treatments we have investigated will impact the performance of the fuel cell that incorporates them. The rationale for restructuring the membrane–electrode interface is to increase the volume of the interface and promote better access for the reacting species leading to reduced ohmic and activation overpotentials. However, restructuring can also lead to increased methanol crossover from a thinner membrane which would in turn lead to higher overpotentials.

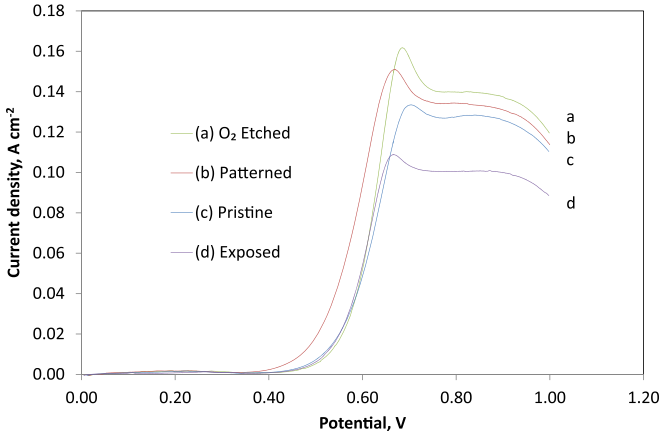

Fig. 8. Methanol crossover measurements for (a) O_2-etched, (b) patterned, (c), pristine and (d) exposed Nafion 212 membranes.

3.8. Performance characterization of fabricated N212 membrane

Fig. 9a shows the polarization curves for exposed, O_2-etched, pristine, and patterned Nafion 212 membranes. It is apparent that

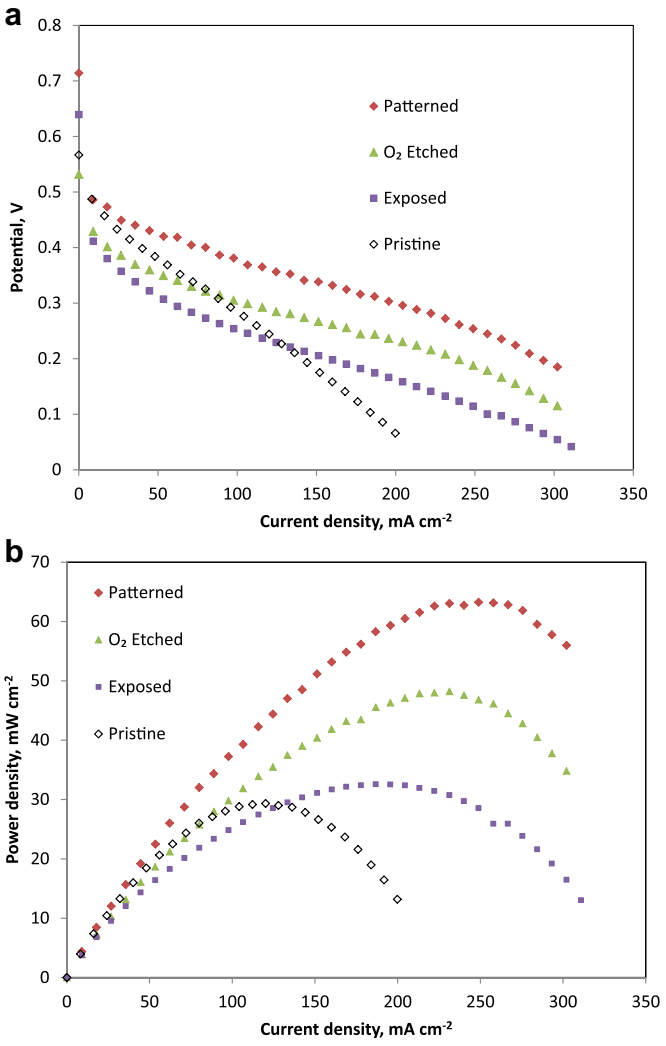

Fig. 9. Polarization (a, upper) and power (b, lower) plots of pristine, O_2-etched, exposed, and patterned Nafion 212 membranes.

Table 2
Summary of in-situ performance characterization results for tested Nafion membranes.

Membrane	Area-specific resistance, mΩ cm^2	Methanol crossover current, mA cm^{-2}	Current density at 0.2 V, mA cm^{-2}	Maximum power density, mW cm^{-2}
Pristine N212	120.1	120.1	136.2	29.3
O_2-etched N212	81.1	145.6	232.2	48.2
Ebeam exposed N212	93.3	108.8	142.2	32.5
Patterned N212	86.1	135.9	284.2	63.1
Pristine N117	270.6	87.6	240.0	50.1

the pristine membrane had the largest polarization requirement for current production. Consistent with the observation in Fig. 7, the pristine membrane exhibited a larger resistance. The corresponding power curves are shown in Fig. 9b. The patterned Nafion 212 membrane exhibited the best performance, while its pristine counterpart (N212) exhibited the worst performance. For the tested membranes, the maximum power typically occurs around 0.2–0.3 V. At a cell voltage of 0.2 V the current densities were 136.2, 142.2, 232.2, 284.2 mA cm^{-2} for the pristine, exposed, etched, and patterned membranes respectively. This is indicative of more efficient catalyst utilization by the patterned membrane. At current densities between 0 and 100 mA cm^{-2}, the pristine membrane had a better performance compared to the exposed membrane. Over the entire current range, the maximum power densities were 29.3, 32.5, 48.2, and 63.1 mW cm^{-2} for the pristine, exposed, etched, and patterned membranes respectively. The performance results are summarized in Table 2.

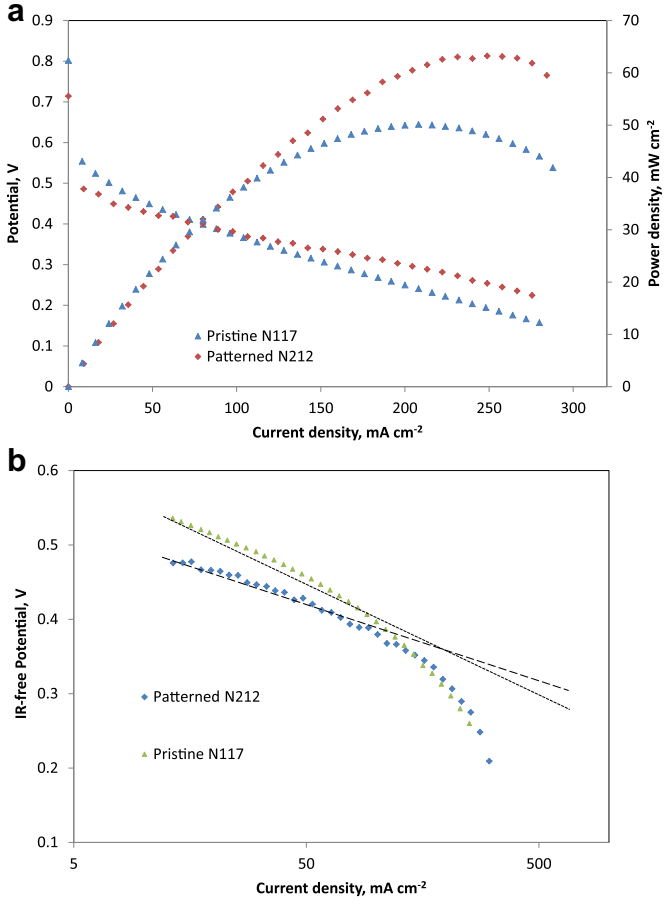

Fig. 10. Performance (a, upper) and Tafel (b, lower) plots of pristine 117 and patterned 212 Nafion membranes.

With the exception of the patterned cell, the trend in open circuit potential for the tested cells in Fig. 9b is consistent with the methanol crossover data from Fig. 8. It would appear that the patterning disrupts the reduced OCV that results from the mixed potential caused by methanol crossover. This will be the subject of continued research to elucidate the effect of the interfacial structure created by ebeam patterning on performance. However, it can be concluded from the power plot (Fig. 9a) that the structured cells, i.e., etched and patterned, perform better than the planar cells.

Although the Nafion 212 membrane is known for its superior conductance, Nafion 117 is more typically used for DMFC applications because of its lower methanol permeability. Thus, a Nafion 117 MEA was prepared from the same GDEs as the patterned MEA and was likewise hot-pressed at the same conditions in order to compare the two membranes. Fig. 10a shows the polarization and power density plots for the patterned Nafion 212 and pristine Nafion 117. Nafion 117 is approximately 3.5 times thicker than the N212 sample, and clearly has a higher ohmic resistance. From the current interrupt measurement, a resistance of 270 mΩ cm^2 was obtained for the N117. This is approximately three times the resistance of the patterned membrane. A methanol crossover current density of 87.6 mA cm^{-2} was obtained for the N117 from linear voltammetry measurements. This is in agreement with the higher open circuit potential shown in Fig. 10a. The resulting maximum power density from the polarization studies was 50.1 mW cm^{-2} for the 117 compared to 63.1 mW cm^{-2} for the patterned 212 sample. At first inspection, it appears the difference in performance is only due to the increased conductivity of the patterned 212 membrane, but the more significant activation loss in the pristine 117 cell also contributes. Fig. 10b shows the Tafel plot for patterned N212 and pristine Nafion 117. The Tafel slope was calculated from the linear region between 10 and 100 mA cm^{-2}. The slopes were 105.5 mV dec^{-1} and 151 mV dec^{-1} for the patterned N212 and pristine N117 membranes respectively. This difference is attributed to the enlarged interfacial area of the patterned membrane.

The key differences between the pristine N117 and patterned N212 cells are membrane thickness and membrane–electrode interfacial structure. As shown in Fig. 9a, b, and 10a, reduced thickness and consequently resistance of the pristine N212 cell cannot overcome the deleterious methanol crossover effect and performs worse than the N117 cell. Thus the significant boost in performance can strongly be attributed to the benefits of the interfacial restructuring via ebeam lithography and dry etching.

4. Conclusion

We present the performance evaluation of electron beam patterned Nafion 212 membrane for DMFC applications. Pristine, O_2 blanket-etched, ebeam exposed and patterned Nafion 212 membranes were compared. Several parameters including in-plane conductivity, methanol crossover, and through-plane ohmic resistance were evaluated. The patterned membrane had the best

combination of properties, benefiting from exposure to the electron beam and interfacial area augmentation as evidenced by its superior power density. To assess performance against a more standard membrane for DMFC use, a Nafion 117 membrane test cell was also compared. While it exhibited reduced methanol crossover, it also had higher ohmic resistance and Tafel slope. The patterned Nafion 212 provided a 25% increase in performance compared to the N117 membrane.

Electron beam lithography coupled with dry etching provides a route to fabricating arbitrary nano/micro patterns in Nafion. It is envisioned that with the extension to Nafion 117 membranes and further optimization, this would lead to the deployment of DMFC cells with tailored properties and significant performance enhancement.

Acknowledgements

The authors are grateful to Dr. Aaron Stein and Dr. Ming Lu for their help with the electron beam lithography, dry etching and sputter deposition tools at Brookhaven National Laboratory. The fabrication work was performed at the Center for Functional Nanomaterials, Brookhaven National Laboratory, which is supported by the U.S. Department of Energy, Office of Basic Energy Sciences under contract No. DAC0298CH10886.

References

[1] V. Neburchilov, J. Martin, H. Wang, J. Zhang, Journal of Power Sources 169 (2007) 221–238.
[2] M. Ahmed, I. Dincer, International Journal of Energy Research 35 (2011) 1213–1228.
[3] J. Larminie, A. Dicks, Fuel Cell Systems Explained, J. Wiley, West Sussex, 2003.
[4] M.H. Yildirim, J. te Braake, H.C. Aran, D.F. Stamatialis, M. Wessling, Journal of Membrane Science 349 (2010) 231–236.
[5] W. Grot, Flourinated Ionomers (Plastic Design Library Fluorocarbon), William Andrew, New York, 2007.
[6] A.A. Kulikovsky, Journal of Electrochemical Society 152 (2005) A1121.
[7] Y. Zhang, J. Lu, H. Zhou, T. Itoh, R. Maeda, Journal of Microelectromechanical Systems 17 (2008) 1020–1028.
[8] L.J. Hobson, H. Oozu, M. Yamaguchi, S. Hayase, Journal of New Materials for Electrochemical Systems 5 (2002) 113–122.
[9] W.C. Choi, J.D. Kim, S.I. Woo, Journal of Power Sources 96 (2001) 411–414.
[10] A. Omosebi, R.S. Besser, Journal of Electrochemical Society 158 (2011) D603–D610.
[11] H. Helvajian, Microengineering Aerospace Systems, Aerospace Press (1999).
[12] J.H. Kim, J. Sohn, J.H. Cho, M.Y. Choi, I.G. Koo, W.M. Lee, Plasma Processes and Polymers 5 (2008) 377–385.
[13] K. Kunimatsu, B. Bae, K. Miyatake, H. Uchida, M. Watanabe, The Journal of Physical Chemistry B 115 (2011) 4315–4321.
[14] D.T. Hallinan Jr., Y.A. Elabd, The Journal of Physical Chemistry B 113 (2009) 4257–4266.
[15] H.J. Humecki, Practical Guide to Infrared Microspectroscopy, M. Dekker, 1995.
[16] N.N. Li, A.G. Fane, W.S.W. Ho, T. Matsuura, Advanced Membrane Technology and Applications, John Wiley & Sons, 2008.
[17] F. Barbir, S. Yazici, International Journal of Energy Research 32 (2008) 369–378.
[18] K.R. Cooper, Journal of Electrochemical Society 157 (2010) B1731.